Biocompatible humidity sensor using paper cellulose fiber/GO matrix for human health and environment monitoring

Khan, Muhammad Umair; Abbas, Yawar; Abunahla, Heba; Rezeq, Moh'd; Alazzam, Anas ; Alamoodi, Nahla ; Mohammad, Baker

DOI
10.1016/j.snb.2023.134188

Publication date
2023

Document Version
Final published version

Published in
Sensors and Actuators B: Chemical

Sensors & Actuators: B. Chemical 393 (2023) 134188

Contents lists available at ScienceDirect

Sensors and Actuators: B. Chemical

journal homepage: www.elsevier.com/locate/snb

Biocompatible humidity sensor using paper cellulose fiber/GO matrix for human health and environment monitoring

Muhammad Umair Khan [a,b], Yawar Abbas [b,c], Heba Abunahla [d], Moh'd Rezeq [b,c], Anas Alazzam [b,e], Nahla Alamoodi [b,f,*], Baker Mohammad [a,b,*]

[a] Department of Electrical Engineering and Computer Science, Khalifa University, Abu Dhabi 127788, United Arab Emirates
[b] System on Chip Lab, Khalifa University, Abu Dhabi 127788, United Arab Emirates
[c] Department of Physics, Khalifa University, Abu Dhabi 127788, United Arab Emirates
[d] Department of Quantum and Computer Engineering, TU Delft, The Netherlands
[e] Department of Mechanical Engineering, Khalifa University, Abu Dhabi 127788, United Arab Emirates
[f] Department of Chemical Engineering, Khalifa University, Abu Dhabi 127788, United Arab Emirates

ARTICLE INFO

Keywords:
Cellulose
Humidity sensor
Graphene sensor
Paper sensor
Biodegradable sensor

ABSTRACT

Environmentally friendly humidity sensors with high sensing performance are considered crucial components for various wearable electronic devices. We developed a rapid-response and durable Paper Cellulose Fiber/Graphene Oxide Matrix (PCFGOM) humidity sensor using an all-carbon functional material. The fabricated sensor demonstrated a high sensitivity to humidity through an electrical impedance measurement, with an increase in response to humidity ranging from 10% to 90% at 1 kHz and 10 kHz, respectively, along with a response time of 1.2 s and a recovery time of 0.8 s. The stability of the sensor was also examined, with consistent performance over a period of 24 h. This novel sensor was employed in several applications, including non-contact proximity sensing, environmental humidity detection, and human respiration detection, to showcase its potential. Moreover, this work represents a significant milestone in developing inexpensive and eco-friendly humidity sensors, given the abundance of paper and graphene in nature and their biocompatibility.

1. Introduction

Humidity sensors are widely utilized in a variety of industries, including environmental monitoring, automotive defogging, respiratory monitoring, manufacturing line monitoring, agricultural and forestry breeding, weather detection, food logistics, and wearable flexible equipment [1–3]. Making humidity sensors more sensitive, responsive, and hysteresis-free is currently a major research focus [4–6]. The fabrication and design of humidity sensors can be accomplished using a variety of transduction techniques, such as optical fiber, capacitance [4], resistance [5], surface acoustic wave [6], field effect transistor [7], quartz crystal microbalance [8], and gravimetric [9–11]. Additionally, humidity sensors use a variety of detecting materials, such as polymers [12], transition metal dichalcogenides[5], bio-membranes[13], metal oxides [14], and composites [15]. Nonetheless, each has its own set of advantages and applications. For example, humidity-sensing materials deposited on flexible substrates, including polyimide, polydimethylsiloxane, polyethylene terephthalate, and polyethyleneimine, are often used in wearable electronics [5,14,16]. As long as there is weak interfacial interaction between the substrate, the conductive fillers, and the humidity sensing layer, their separation is likely to occur during the deformation process, which leads to poor performance in wearable electronics [5,17,18]. These synthetic polymer substrates are not biodegradable, which invariably causes environmental pollution [2,19,20]. Using green and eco-friendly materials for device manufacturing would considerably reduce the environmental effect of such device development while maintaining high-performance functionality [13,19,21,22]. Biodegradable, biocompatible, nontoxic, and renewable paper cellulose is the most abundant natural polymer [2,20,23]. Due to its mechanical/chemical stability, high hydrophilicity, abundance of hydroxyl groups, and water insolubility, paper cellulose is regarded as a promising candidate for developing humidity sensors [1–3,20,23]. However, cellulose lacks one crucial sensor property, namely, its electrical conductivity [2,3,20].

Therefore, much effort has been put into integrating carbon-based conductive materials because of their high conductivity and stability

* Corresponding authors at: System on Chip Lab, Khalifa University, Abu Dhabi 127788, United Arab Emirates.
E-mail addresses: Nahla.alamoodi@ku.ac.ae (N. Alamoodi), baker.mohammad@ku.ac.ae (B. Mohammad).

https://doi.org/10.1016/j.snb.2023.134188
Received 20 April 2023; Received in revised form 14 June 2023; Accepted 14 June 2023
Available online 20 June 2023

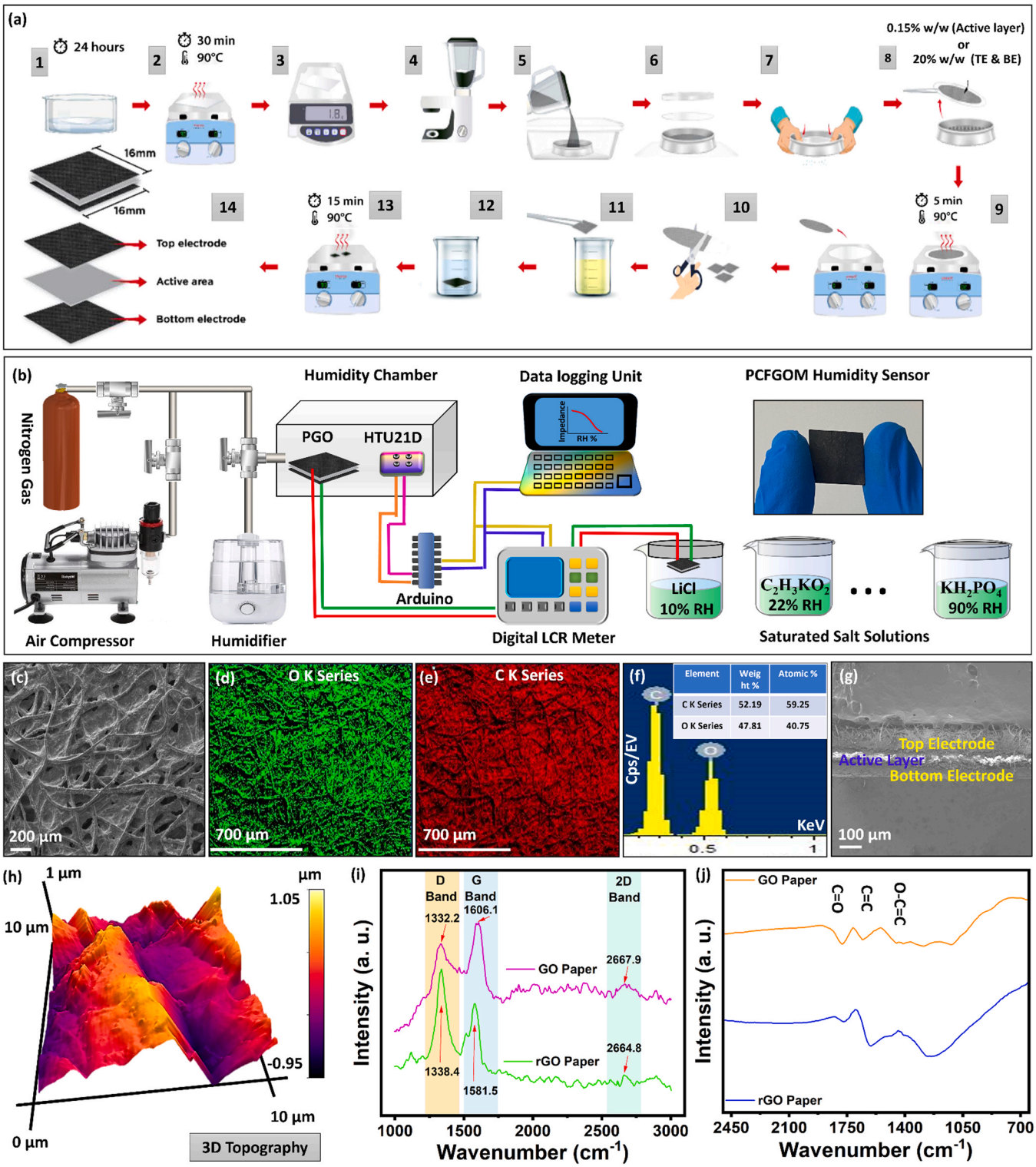

Fig. 1. (a) Fabrication process of humidity sensor. (b) The schematic of the fabricated sensor and Experimental setup used for the electrical measurements of the sensor. (c) The SEM image of rGO sensing layer at scale bar of 200 µm. The EDS color mapping shows (d) O K series and (e) C K series. (f) The EDS profile showing peaks of C and O and weight % and atomic %. (g) The cross-sectional image of the fabricated humidity sensor. (h) 3D topography of the sensing layer. (i) Raman Spectrum of GO, and rGO. (j) FTIR spectrum of GO, and rGO paper.

for humidity sensors in composite or layered structures using cellulose and paper substrates [2,23]. For example, nano-cellulose graphene-based humidity sensors, carbon nanotube graphene-based humidity sensors, and graphene nanoplatelets cellulose nanofiber-based humidity sensors have been proposed via spray coating, dip coating, filtration method, and screen printing, respectively [2,3,20]. The strong water affinity of cellulose gave the as-prepared sensor substantial humidity detection capabilities [2,23]. Moreover, the incompatibility and poor affinity between the stiff conductive filler and flexible paper cause cracking during the deformation process, which affects device performance and stability [2,20,23]. To address these issues, in this work, novel fabrication process is introduced to fabricate the biocompatible

humidity sensor using Paper Cellulose Fiber/Graphene Oxide Matrix (PCFGOM) blend at different weight/weight(w/w) ratios to improve the device detection range and linearity, flexibility, stability, transient response for environment monitoring and human health monitoring. Gong et al. [2] report cellulose nanofiber and dispersed graphene-filtered film for humidity response, displaying an improved sensitivity of 15–99% RH but a relatively slow response time (45 s) and recovery time (33 s). Yoshida et al. [3] report cellulose nanofiber and graphene nanoplatelet composite as a sensing layer and electrode (interdigital electrodes), with a 30–90% RH sensing range and an improved response and recovery time of 17 s and 22 s, respectively. Kafy et al. [1] report cellulose nanocrystal/GO composite film on interdigital electrodes with a humidity sensing range of 30–80% RH, and response time of 90 s, and a recovery time of 30 s. Yang et al. [24] report nano-fibrillated cellulose/graphene oxide/polydimethylsiloxane aerogels via freeze drying on interdigital electrodes. The sensor response is highly nonlinear in the range of 11–97% RH with a response time of 57 s and a recovery time of 2 s. Despite the advancements in design and achievements, several issues still need to be addressed, such as poor sensing results, slow response, recovery time, sensor linearity, and a difficult fabrication process. Herein, we propose a rapid-response durable humidity sensor employing a PCFGOM structure. The concentration of GO in the electrodes and active layer is 20% w/w and 0.15% w/w, respectively. The humidity sensor is immersed in Hydriodic (HI) acid for the necessary time to convert GO to reduce graphene oxide (rGO) to fine-tune the electrical conductivity. The PCFGOM humidity sensor demonstrated a quick response of 1.3 s and recovery time of 0.8 s, low hysteresis, a wide RH detection range between 10% and 90% at 1 kHz and 10 kHz, and sensor stability analyzed for more than 24 h. The sensor also has the ability to detect human breathing, measure humidity in the surrounding environment, and non-contact proximity sensing.

2. Experimental section

2.1. Materials

A simple and inexpensive method is used for the fabrication of the PCFGOM humidity sensor. For the fabrication of the humidity sensor, standard copy paper and graphene oxide dispersion in water at a concentration of 4 mg/mL (2.5 wt percentage, Graphene, San Sebastian, Spain) are the primary materials used. A schematic of the fabrication method for the PCFGOM humidity sensor is shown in Fig. 1(a).

2.2. Sensor fabrication

The detailed fabrication process is discussed in our previously reported work [25]. To eliminate any water-soluble pollutants linked to the paper and to liberate its fibers, the first step entails soaking common copy paper in a deionized (DI) water bath for 24 h. After drying the soaked paper on a hot plate for 30 min at 90 °C the weight of the dry paper is measured using a weighing scale. The paper is then ground into a pulp in DI water using a blender, and a predetermined volume of GO solution is added. The required GO concentration determines the volume of the GO solution (the weight of paper ratio to the weight of GO). The paper-GO-deionized water pulp is then mixed for 2 min for smooth consistency. The initial layer of the device is constructed with a high GO concentration to act as a top and bottom electrode (20% w/w). To achieve this the pulp is then poured into a laboratory sieve set, which is placed in a DI water-filled container. The pulp is dispersed uniformly over the sieve surface to make a consistent paper film. Following that, the sieve is carefully lifted from the container. To press and drain water from the sieve while releasing the pulp in the form of a paper disc, the pulp is covered with an overhead projector (OH) film and a 1 cm thick plexiglass disk carefully carved to meet the sieve dimensions. The disk is then removed, and the paper layer detaches from the sieve while still attached to the OH film. The OH film with the attached layer is baked for 5 min at 90 °C on a hot plate, completing the top electrode fabrication. The same processes as in steps 1–9 is performed to create the active layer, but with a different weight ratio of GO (0.15% w/w in this work), as illustrated in Fig. 1(a). The stacking of the layers for PCFGOM humidity sensor as 20% w/w GO paper cellulose fiber matrix as top and bottom electrode and 0.15% w/w GO paper cellulose fiber matrix as active layer. After 20 min of heating the sensor on a hot plate at 90 °C, the sensor is removed, and the three layers of paper are cut to the required size. The humidity sensor is then submerged in HI acid for a predetermined time to convert GO to its reduced form rGO, which allows for fine-tuning electrical conductivity. Following that, the sensor is completely cleansed in DI water multiple times using numerous fresh DI baths. In the final step, the devices are baked for 15 min on a hot plate heated to 90 °C. The three-layered sensor devices are presently operational. Fig. 1(a) depicts an exploded view of the three layers and a schematic representation of the PCFGOM humidity sensor device.

2.3. Sensor material characterization

A field emission scanning electron microscope (FESEM), model JSM-7610 F from JEOL, was used to take microphotographs, EDS color mapping, and element maps of the fabricated humidity sensor device. The ASYLUM MFP-3D's atomic force microscope (AFM) was used to examine the sensor's surface roughness in its AC mode topography[26, 27]. A high-frequency silicon tip of resonance frequency ~256 kHz with a 30 nm apex diameter was employed for the topography of the sensor. GO, and rGO quality in the devices are being examined using Raman spectroscopy to confirm the presence of rGO. Fourier Transform Infrared (FTIR) spectroscopy was carried out using a Bruker Alpha system fitted with a diamond reflectance accessory to analyze the functional groups.

2.4. Sensor evaluation setup

The electrical behavior of the PCFGOM humidity sensor was studied across a wide range of RH values. As shown in Fig. 1(b), saturated solutions of various salts (LiCl, $C_2H_3KO_2$, $MgCl_2$, NaBr, NaCl, and KH_2PO_4) were put in airtight glass jars to provide a variety of humidity conditions at 25 °C (room temperature). The varying relative humidity (RH) values produced by these saturated aqueous solutions were 10%, 22%, 33%, 57%, 76%, and 90% RH. The RH values of the various salt solutions maintain accuracy between 1% and 2% RH, depending on the environment's temperature and the salt used. The % RH of several salt solutions was calculated using a commercial HTU21D sensor and an Arduino UNIO unit. The proposed humidity sensor's capacitance and impedance responses to relative humidity were measured using a GOWE LCR meter (AT826). The sensor's electrical readings were all made at 25 °C. The LCR meter and Arduino UNO were directly linked to the computer for data logging. The sensor range, stability, hysteresis, and application (non-contact sensing, human breath monitoring, and environment monitoring) were measured in the air environment (as a base gas). Evaluation of the transient response involved using a humidifier, air compressor, and nitrogen gas.

3. Results and discussion

3.1. Material characterization

A field emission scanning electron microscopy (FESEM) analysis is performed for the proposed humidity sensor. Fig. 1(c) shows a low-magnification FESEM image of PCFGOM humidity sensor electrodes. It is noticeable that the GO flakes create a coating film within the microfibers, bonding them together. The elemental color mapping shows the carbon C-K series and oxygen O-K series, as shown in Figs. 1(d) and 1(e), evidencing the presence of carbon and oxygen. The elemental composition shows the carbon and oxygen peaks with weight % of 52.19 and 47.81, respectively, as shown in Fig. 1(f). An analysis of the PCFGOM

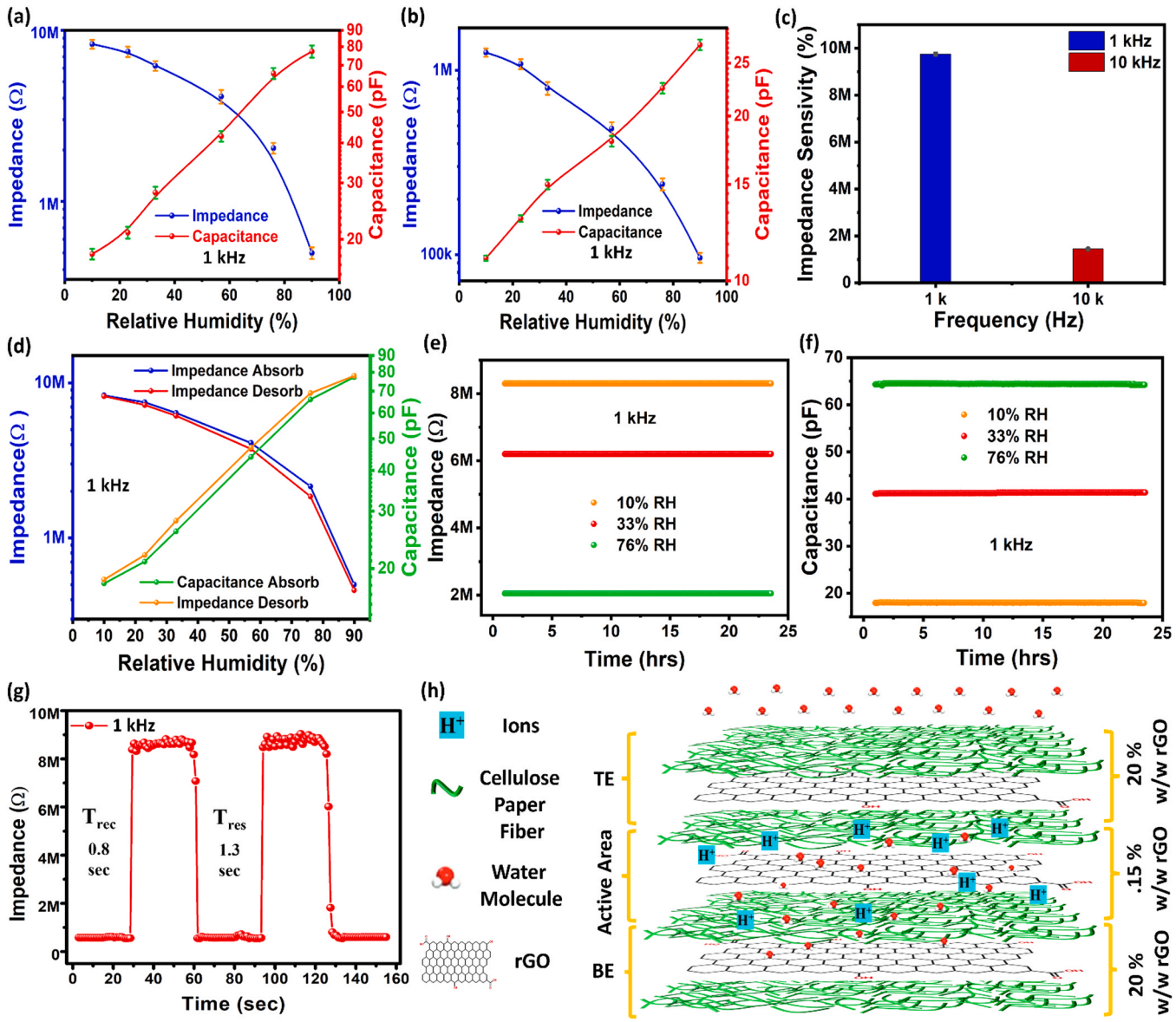

Fig. 2. The humidity sensor's impedance and capacitance responses (a) 1 kHz and (b) 10 kHz frequency. (c) Sensitivity of the fabricated sensor. (d) Sensor response to humidification and dehumidification cycle. Stability test analyzed for 24 hrs to monitor (e) impedance, and (f) capacitance. (g) The humidity sensor's impedance transient response times at 1 kHz. (h) Illustration of the humidity sensing mechanism.

humidity sensor's three layers' bonding is done using a cross-section FESEM image, as seen in Fig. 1 (g). According to FESEM measurements, the tested device has a thickness of around 350 μm. Further, AFM is used to analyze the surface at a magnified scale with root mean square roughness ~ 600 nm, as shown in 3D topography images in Fig. 1 (h).

Fig. 1(i) displays the Raman spectra for two different samples that include GO before and after reduction. Both devices exhibit two prominent vibrations in the 1000 cm^{-1} to 3000 cm^{-1} range. The breathing mode of j-photons with A1g symmetry is connected with the D-vibration band[28]. With GO, and rGO paper, the D-band occurred at 1332.2 cm^{-1}, and 1338.4 cm^{-1}, respectively. When the number of defects in the graphene plane increases, the D band's intensity rises. As a result, when the oxygen functionalities are removed, the graphene plane develops defects[22], as seen in Fig. 1(i), which causes the D-band to rise. The G-vibration band, which depicts the first order E2g optical mode of the C-C double bond of the graphite plate, occurred at 1606.1 cm^{-1} for GO paper and 1581.5 cm^{-1} for rGO paper[28]. As more oxygen groups are present in GO, the location of the G-band moves to a higher wave number, while during the reduction process, the G-band shifts to a lower frequency, as shown in Fig. 1(i) for the rGO sample, and it agrees with the results in the literature[22,28–30]. The disorder and tangential bands, respectively, are shown by the D and G-bands. Moreover, for GO paper, and rGO paper, the 2D band was seen at 2667.9 cm^{-1} and 2664.8 cm^{-1}, respectively[22]. The graphene layer may be identified using this band because it is sensitive to the stacking of graphene layers. The ID/IG ratio may also be used to represent the defects in the GO structure[22]. In the case of rGO, the ID/IG ratio increased from 0.99 to 1.06. This is primarily due to decreasing sp^2 domain sizes and the restoration of sp^2 carbon following reduction. The findings confirm the existence of rGO and match the data provided in the literature. To measure the deoxygenation of GO, FTIR spectra, as shown in Fig. 1(j), have been studied. One of the most notable features of pristine GO samples is the presence of a rich collection of transmission bands that correspond to oxygen carbon groups (OCGs) for example, C═O at 1730 cm^{-1}, O–C═O around 1389 cm^{-1}[22]. After reduction, the majority of them disappeared, implying that OCGs were effectively removed[22], as shown in Fig. 1(j).

Table 1
Performance parameter comparisons between the fabricated sensor and those described in the literature for other sensors based on 2D materials, GO, Graphene and CNT.

Humidity Sensing Materials	Detection Range RH %	Response Time (sec)	Recovery Time (sec)	Curve Shape	Sensing Principle	Ref.
WS_2	40–80	13	17	Almost Linear	Resistive	[35]
$TiSi_2$	0–100	0.9	8	Linear	Impedance & Capacitance	[31]
$ZrSe_2$	15–80	1	2	Linear	Impedance & Capacitance	[32]
MoS_2	0–60	9	17	——	Resistive	[36]
VS_2	0–100	40	50	Almost Linear	Resistive	[37]
PSS-Graphene	30–95	3	22	Almost Linear	Impedance	[38]
ZnO	0–97	6.2	9.6	Non-linear	Gravimetric	[39]
GO/In_2O_3	11–97	15	2.5	Non-linear	Capacitance	[40]
SnS_2/GO	0–97	6	15	Non-linear	Resistive	[41]
GO	20–90	0.8	2.4	Non-linear	Potentiometric	[34]
GO	10–90	15.8	–	Non-linear	Capacitance	[42]
GO	8–95	3	7.7	Non-linear	Resistive	[43]
PDDA/GO	6–66	300	147	Non-linear	Resistive	[44]
GO	11–97	94	134	Linear	Resistive	[45]
GO	2–90	–	–	Almost Linear	QCM	[46]
GO	6–97	45	24	Non-Linear	QCM	[47]
GO/PEI	11–97	53	18	Non-linear	QCM	[48]
GO	25–65	5	–	Non-linear	Capacitive	[49]
GO-Si Bilayer	10–98	19	10	Almost Linear	Voltage	[50]
CNT Cellulose	10–95	321	435	Linear	Current	[20]
CNT Cellulose	11–95	333	523	Linear	Current	[23]
GO Fiber	10–65	–	–	Non-linear	Current	[33]
GO	11–97	54	12	Non-linear	Acoustic	[51]
GO	10–90	7	13	Almost Linear	Gravimetric	[52]
GO	10–90	3	10	Non-linear	Gravimetric	[53]
GO	10–90	10	10	Almost Linear	Gravimetric	[54]
GO	10–90	6	–	Non-linear	Gravimetric	[55]
Graphene Cellulose Paper	30–90	1	6	Linear	Resistive	[19]
Cellulose Nanofiber Graphene	15–99	45	33	Almost Linear	Resistive	[2]
Cellulose Nanofiber/ Graphene Nanoplates	30–90	17	22	Nonlinear	Resistive	[3]
Cellulose Nanocrystal/GO	30–80	90	30	linear	Capacitive	[1]
Nanofibrillated cellulose/GO/PDMS aerogel	11–97	57	2	Non-Linear	Capacitive	[24]
PCFGOM	**10–90**	**1.3**	**0.8**	**Linear**	**Impedance & Capacitance**	**This work**

3.2. Electrical response

The impedance and capacitance responses of the PCFGOM humidity sensor were analyzed at test frequencies of 1 kHz and 10 kHz under various humidity levels (0% to 90% RH) to examine the electrical performance of the proposed humidity sensor. Impedance is a metric for determining a circuit's resistance and reactance. On the other hand, capacitance indicates the material's capacity to hold an electrical charge. Due to the presence of water molecules, PCFGOM humidity sensor impedance and capacitance may change. A hygroscopic expansion of the sensing layer under humid conditions further amplifies electrical signals. The paper cellulose fiber supplied a lot of adsorption sites (-OH, -COOH) to collect water molecules at the same time as it served as a reservoir. As a result, water molecules that had been absorbed transferred more electrons to the active layer. Thus, the impedance and capacitance of the sensor vary when the humidity level changes. Fig. 2(a-b) show the impedance and capacitance responses at 1 kHz and 10 kHz, respectively. The findings in Fig. 2(a), indicate that the impedance changed linearly from 8.3 MΩ to 500 KΩ with a change in RH from 10% to 90% during the 1 kHz test frequency. As the relative humidity increases, the sheet resistance of the active layer decreases, causing the impedance to drop. Similarly, the impedance at 10 kHz frequency begins at 12.5 MΩ at 10% RH and then declines linearly with the rise in relative humidity, finally falling to 96 kΩ at 90% RH, as shown in Fig. 2(b). The linearity of the response at test frequencies of 1 kHz and 10 kHz indicates that the PCFGOM humidity sensor has a 10–90% RH detection limit that can be monitored appropriately. As a result of the water molecule's higher polarization at low frequencies, the active layer and the water molecules experience stronger electrostatic attractive forces. Therefore, the impedance shift at low frequencies (1 kHz) is more noticeable than at higher frequencies (10 kHz). The (H^+) ions generated by the water molecules cannot keep up with the alternating rate of the applied electric field because the electric field varies fast at the high-test frequencies. This led to a weak dielectric property that was less sensitive to humidity. At 1 kHz and 10 kHz, the suggested sensor's impedance sensitivity (S_Z) is 9750000% and 1442500%, as shown in Fig. 2(c), calculated from Eq.(1) [5]. Zl and Zu represents the impedance at higher relative humidity levels (RHu) and lower humidity level (RHl).

$$SZ = \frac{Zu - Zl}{RHu - RHl} \times 100 \quad (1)$$

The PCFGOM humidity sensor capacitance behavior was also assessed in response to variations in relative humidity. The water molecules absorption in the active region causes the permittivity of the sensing layer to rise as the RH increases. As shown in Fig. 2(a), at 1 kHz. The measured capacitance was 18 pF at 10% RH, which continues to rise, reaching 77 pF at 90% RH. In addition, at 10 kHz, the capacitance response starts at 11 pF at 10% RH and increases to 27 pF at 90% RH, as shown in Fig. 2(b). The relative permittivity of the sensing medium decreases as the relative humidity increases, and therefore the device's capacitance increases. According to the given formula $C = (\kappa\varepsilon_0 A)/d$, where κ is the dielectric constant and its value increases with the increase in humidity level. The humidity level was scaled up from 10% to 90% RH , then decreased down from 90% to 10% RH using saturated salt solutions to create the adsorption and desorption cycles for which the sensor's impedance and capacitance were both recorded. Charges injected from the interfaces between electrodes and the active layer are trapped in molecular gaps, which results in hysteresis[27,31], as shown in Fig. 2(d). When placed in an electric field, water molecules may align

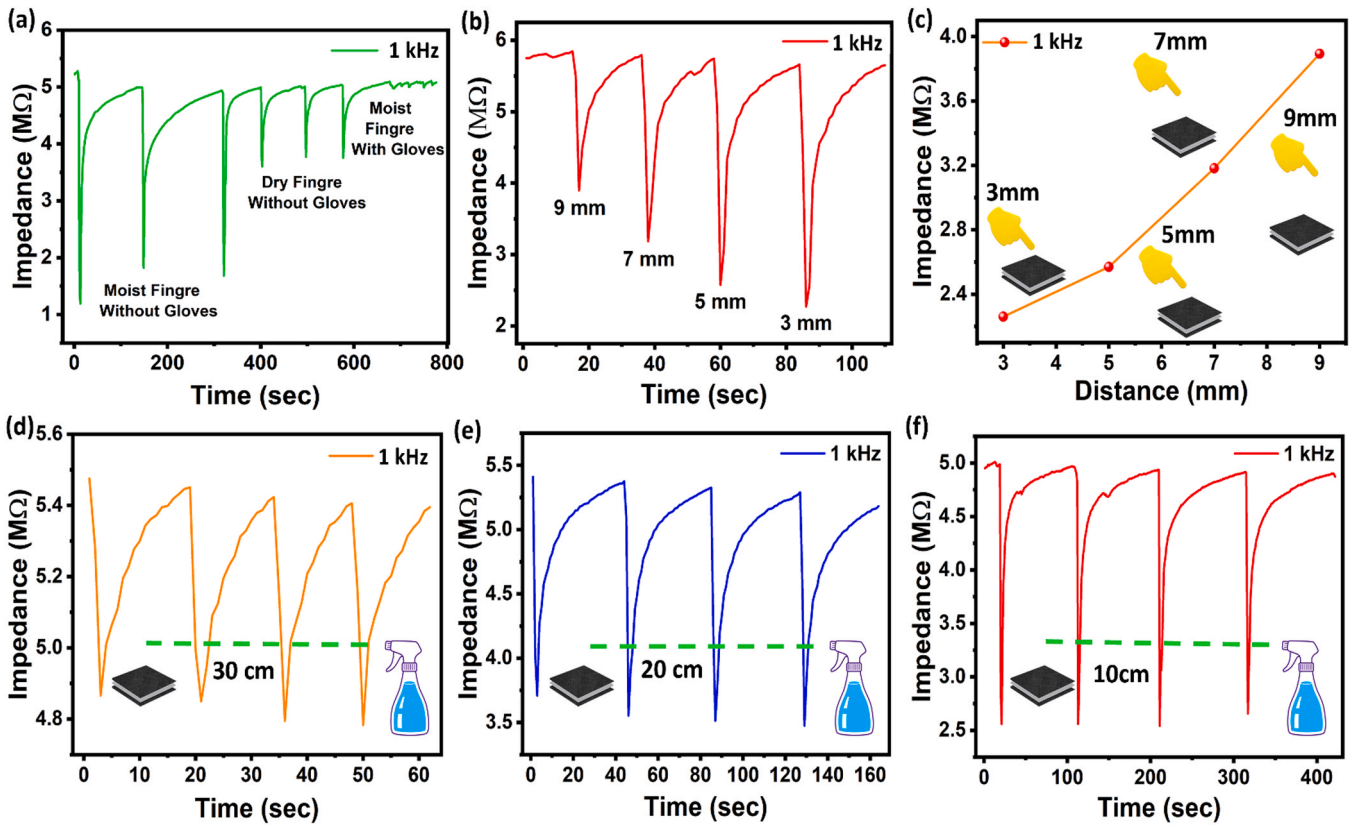

Fig. 3. (a) Impedance curves for non-contact sensing of a moist finger without and with gloves, as well as a dry finger without gloves. (b) The non-contact humidity sensing test with finger proximation test at different distances in a range of 9–3 mm. (c) The impedance change of PCFGOM humidity sensor for non-contact sensing at different distances in a range of 9–3 mm. The capacitance behavior of the proposed sensor, while spraying water from the atomizer at a given distance of (d) 30 cm, (e) 20 cm, and (f) 10 cm.

to create polar molecular structures thanks to their large electric dipole ~1.8D[31]. Different charge trap densities are produced by this structural alignment, leading to hysteresis[31]. In addition, the device impedance and capacitance stability were analyzed for 24 h in various humid conditions (10%, 33%, and 76%RH) at 1 kHz frequency, as shown in Fig. 2(e-f), respectively. These results demonstrate that the PCFGOM humidity sensor operation is stable and error-free. Another crucial aspect of a humidity sensor is the transient response time (response and recovery). A humidifier was used to analyze the sensor's response to rapid step changes alternating the RH from 10% to 90% RH, while nitrogen gas and air compressor were used to dehumidify the sample from 90% to 10% RH. Fig. 2(g) displays the measured response and recovery periods for the impedance, which were 1.3 s and 0.8 s, respectively. Repeated impedance humidification and dehumidification cycles demonstrate stable response and recovery durations. These measurements reveal that the suggested sensor has a fast response and recovery time and may be used for real-time practical applications.

3.3. Sensing mechanism

The output (impedance and capacitance) of the humidity sensor was measured, where hydration is controlled by adjusting the external environment's humidity (10–90% RH). The mechanism of the humidity sensor is illustrated in Fig. 2(h). The top and bottom electrodes are highly conductive, and the sandwiched layer has a low GO concentration with high oxygen vacancies. Moreover, the sensing mechanism of the PCFGOM humidity sensor can be explained based on the suggested sensing mechanisms in the literature, which are proton hopping, tunneling, and transfer of electrons from the water molecules on the active sites of the sensing material [32]. At low relative humidity, the H_2O covers the active sites of hydrophilic functional groups such as hydroxyl and carboxyl groups [1,2,23,33]. The rGO paper cellulose fiber matrix electrodes feature a porous structure, that provide a path for H_2O molecules to flow through. The top and bottom electrodes in the PCFGOM humidity sensor, form a conductive pathway, while the active layer serves as a humidity-adsorbing matrix [1,2,20,21,24]. The current flows as a result of the tunneling effect between active water donor sites. In addition, the paper cellulose fiber, which served as a reservoir, offered many adsorption sites (-OH, -COOH) to capture water molecules and encouraged the electron transfer from adsorbed water molecules to the active layer [2,19,22–24]. Increased environmental humidity led to the active layer adsorbing more moisture, which led to a decrease in sensor resistance [1,3,20,24,31]. After water adsorption by the active layer, the hydrogen ion (H^+) was quickly transported from the oxidized end to the reduced end through concentration gradients after being ionized from oxygen-related groups [1,3,31,33,34]. The protons that are mobile are easily accessible for conduction [1,2,23,34]. So, according to Grotthuss's mechanism, proton hopping is the predominant process at high RH [20,22,24,31,33]. When the PCFGOM humidity sensor is linked to an external circuit, the change in impedance and capacitance can be measured. Table 1 compares the various sensing characteristics of PCFGOM humidity sensor with those of previously reported sensors that are based on 2D materials, metal oxides, paper cellulose, GO, Graphene and CNT. The PCFGOM humidity sensor fabricated in this study exhibits a wide operating range, spanning from 10–90% RH, while maintaining a linear response characteristic. Notably, these sensors demonstrate rapid response and recovery times, with values of 1.3 s and 0.8 s respectively. Moreover, PCFGOM humidity sensor exhibit significantly enhanced impedance sensitivity, achieving values of 9750000% and 1442500% at frequencies of 1 kHz and 10 kHz, respectively. Furthermore, the

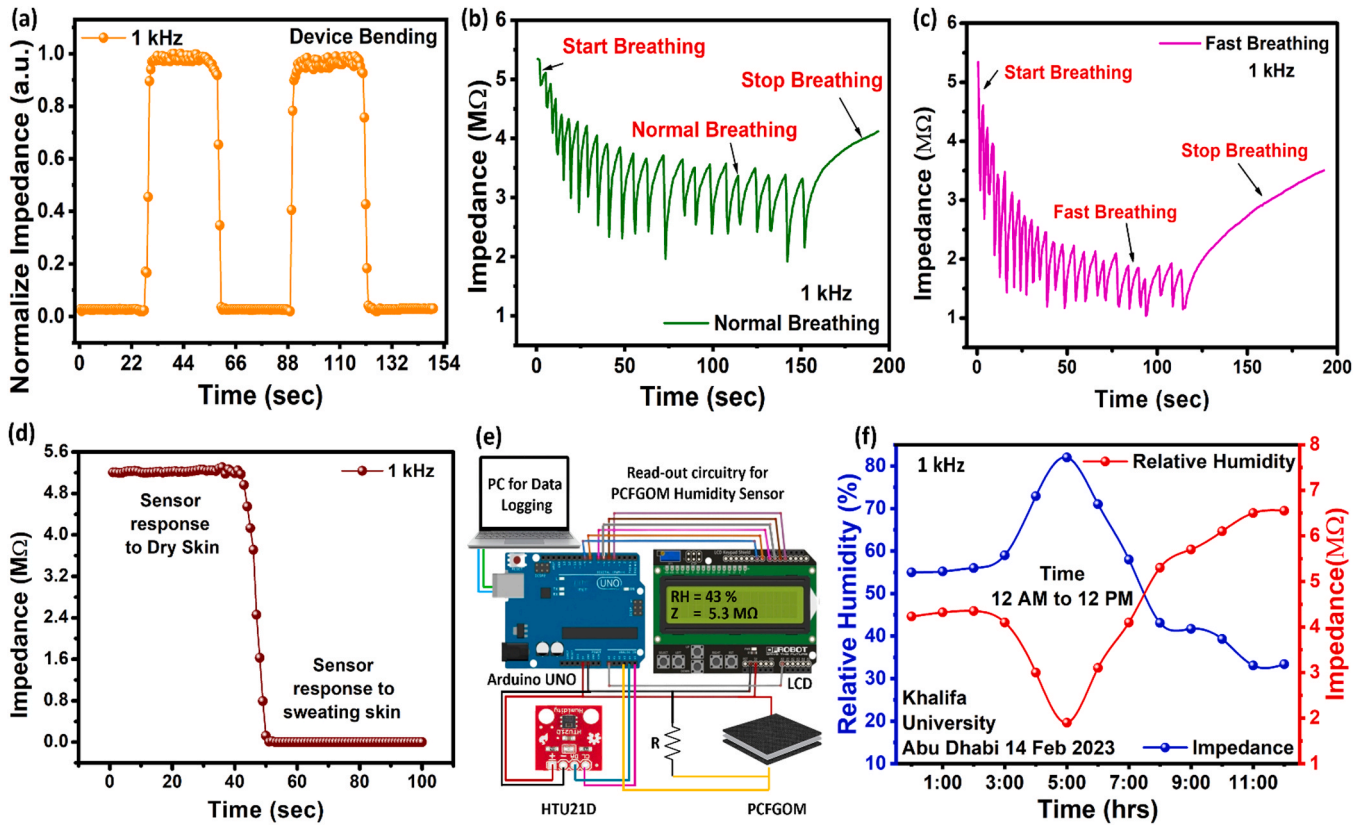

Fig. 4. (a) Bending sensor response and recovery. (b) Breathing test in normal condition and (c) fast breathing condition. (d) Humidity sensor attached to skin to monitor Dry skin and sweating skin response. (e) Read-out circuitry for PCFGOM humidity sensor. (f) Impedance response of fabricated sensor in open environment (data was taken on 14 Feb 2023).

stability of the sensors is diligently monitored for a duration of more than 24 hrs, showcasing consistent and reliable performance throughout the observation period. The outcome demonstrates that the PCFGOM humidity sensor is adaptable to changes in ambient humidity. In contrast to humidity sensors that have been previously reported based on 2D materials, such as GO, graphene, cellulose, paper, and CNT, the comparison between the current work and the previously developed sensors demonstrates that the PCFGOM humidity sensor has an exceptional detection capability, as shown in Table 1.

3.4. Application

Based on its high sensitivity, the PCFGOM humidity sensor was tested for a variety of applications, including the non-contact detection of a human fingertip and water spraying tests at distances of 30 cm, 20 cm, and 10 cm. Fig. 3(a) provides a schematic of human fingertip contactless sensing. After placing the finger 2 mm above the PCFGOM humidity sensor at a frequency of 1 kHz, the sensor displayed an abrupt shift in impedance in response to moist finger humidity at an ambient 40% RH. In the span of 10 s, the impedance curve of a wet finger without gloves rises dramatically from 5.3 MΩ to 1.2 MΩ, as seen in Fig. 3(a). Nevertheless, the dry finger also contains moisture, which causes a fluctuation in the capacitance from 5 MΩ to 4.1 MΩ. Moreover, when we carried out the same test while wearing gloves, there was minimal change in impedance, demonstrating that the PCFGOM humidity sensor solely reacts to humidity, as shown in Fig. 3(a). When a moist finger is placed 3 mm, 5 mm, 7 mm, and 9 mm above the device, the humidity sensor exhibits a quick real-time shift in current, as illustrated in Fig. 3 (b). According to Fig. 3(c), the impedance was determined to be 3.893 MΩ, 3.182 MΩ, 2.57 MΩ, and 2.26 MΩ for distances of 3 mm, 5 mm, 7 mm, and 9 mm, respectively. We also tested the PCFGOM humidity sensor response by spraying water. Initially, the sensor was mounted to the beaker, and water was sprayed from the atomizer at 30 cm, 20 cm, and 10 cm distances from the sensor at ambient 40% RH. For 10 s, water sprayed in the direction of the sensor before abruptly stopping when the impedance returned to its starting point. Impedance changes from 5.4 MΩ to 3.55 MΩ at a distance of 30 cm as shown in Fig. 3(d), from 5.4 MΩ to 4.84 MΩ at a distance of 20 cm as shown in Fig. 3(e), and from 5 MΩ to 2.5 MΩ at a distance of 10 cm Fig. 3(f).

The PCFGOM humidity sensor was used to monitor a person's breathing activities. To track the respiratory reaction, the sensor was positioned within the mask. The sensor's output in this case was detected at 1 kHz. A volunteer wore the mask in normal room conditions. The user was previously given instructions for the apnea phase to test the humidity sensor for different situations. The breathing was divided into two categories: normal breathing and fast breathing as shown in Fig. 4(a-b). The corresponding application of the sensor as normal breathing with an impedance change of ~ 2 MΩ is demonstrated in Fig. 4(a). Fast breathing caused a large change in impedance ~ 1.08 MΩ because more water vapor was expelled under these conditions and was picked up by the sensor, as shown in Fig. 4(b). It was easy to distinguish between the two breathing patterns (slow and fast). The proposed humidity sensor could detect human breathing with appreciable precision and efficacy. Furthermore, the proposed flexible sensor's transient response was measured in a bending state. The sensor is mounted on the bend surface with a diameter of 20 mm. The recorded transient response in the bending state is shown in Fig. 4(c). After the bending test, the proposed sensor delivers good sensing performance with fast response and recovery time by varying the relative humidity from 10% RH – 90% RH by using humidifier and dehumidification is performed using nitrogen gas and air compressor. Furthermore, we adapted the sensor to human skin to monitor the sensor's response to

human sweating. In this case, we attached a PCFGOM humidity sensor to human skin and monitored the sensor response while running. Upon detecting the sweating, the sensor's impedance rapidly decreases from 5.2 MΩ to 530 kΩ, as shown in Fig. 4(d). In order to monitor RH in an open environment, a real-time low-cost read-out circuitry was employed for PCFGOM humidity sensor, as depicted in Fig. 4(e). The prototype consists of an Arduino UNO, HTU21D reference humidity sensor, PCFGOM humidity sensor, voltage divider resistor, LCD 1602 Arduino shield used for visualizing RH and relative impedance change, and a PC used for data logging purposes. The fabricated PCFGOM humidity sensor real-time impedance behavior was analyzed to keep an eye on the outdoor environment (the data was collected at Khalifa University - Abu Dhabi, on February 14, 2023) (midnight to noon). as shown in Fig. 4(f). The relative humidity sensor HTU21D monitors the RH level from midnight to noon. The data is monitored every hour. The proposed PCFGOM humidity sensor demonstrates consistent and stable performance, indicating its potential for real-time monitoring applications.

4. Concluding remarks

We used a straightforward and very effective strategy to produce a high-performance, environment-friendly, disposable paper cellulose fiber/GO matrix humidity sensor. Paper cellulose fibers and graphene oxide matrix composite film were employed for the electrodes as well as the sensing or active layer of the sensor, obviating the necessity for precious metals like silver and gold. For electrodes and active layer, the GO concentration is 20% w/w and 0.15% w/w, respectively. This sensor is eco-friendly since it uses cellulose paper and GO, both of which are widely available in nature, harmless, and affordable. Each layer was combined and stacked to make this paper-based cellulose fiber GO matrix humidity sensor. The sensing characteristics of the sensor were excellent at 1 kHz and 10 kHz frequencies, as it exhibited high impedance sensitivity of 9750000% and 1442500%, respectively. The PCFGOM sensor has fast operating speeds with response and recovery times of 1.3 s and 0.8 s, respectively. Moreover, the sensor's ability to detect moisture from human breath, fingertip proximity, and moisture detection in open environments suggests it has potential utility in agro-industrial enterprises and healthcare systems.

CRediT authorship contribution statement

M.U.K., Methodology, Investigation, Data curation, Visualization, Writing – original draft. **Y.A.**, **M.R.**, Investigation, Data curation, Writing – review & editing. **H.A.**, Validation, Writing – review & editing. **N.A.** Conceptualization, Supervision, Writing – review & editing. **A.A.** Resources, Supervision, Writing – review & editing. **B.M.**, Supervision, Writing – review & editing, Project administration, Resources, Funding acquisition.

Declaration of Competing Interest

The authors declare that they have no known competing financial interests or personal relationships that could have appeared to influence the work reported in this paper.

Data availability

Data will be made available on request.

Acknowledgement

This research is supported by Khalifa University System on Chip Lab grant (RC2-2018-020).

References

[1] A. Kafy, A. Akther, M.I.R. Shishir, H.C. Kim, Y. Yun, J. Kim, Cellulose nanocrystal/graphene oxide composite film as humidity sensor, 2016/08/15/, Sens. Actuators A Phys. vol. 247 (2016) 221–226, 2016/08/15/.
[2] L. Gong, H. Fu, L. Liu, Z. Li, J. Guo, Z. Cao, J. Yao, Construction and performance of a nanocellulose–graphene-based humidity sensor with a fast response and excellent stability, 2022/05/13, ACS Appl. Polym. Mater. vol. 4 (5) (2022) 3656–3666, 2022/05/13.
[3] A. Yoshida, Y.-F. Wang, S. Tachibana, A. Hasegawa, T. Sekine, Y. Takeda, J. Hong, D. Kumaki, T. Shiba, S. Tokito, Printed, all-carbon-based flexible humidity sensor using a cellulose nanofiber/graphene nanoplatelet composite, 2022/04/01/, Carbon Trends vol. 7 (2022), 100166, 2022/04/01/.
[4] F.J. Romero, A. Rivadeneyra, A. Salinas-Castillo, A. Ohata, D.P. Morales, M. Becherer, N. Rodriguez, Design, fabrication and characterization of capacitive humidity sensors based on emerging flexible technologies, 2019/05/15/, Sens. Actuators B Chem. vol. 287 (2019) 459–467, 2019/05/15/.
[5] M. Awais, M.U. Khan, A. Hassan, J. Bae, T.E. Chattha, Printable highly stable and superfast humidity sensor based on two dimensional molybdenum diselenide, 2020/03/26, Sci. Rep. vol. 10 (1) (2020) 5509, 2020/03/26.
[6] X. Le, Y. Liu, L. Peng, J. Pang, Z. Xu, C. Gao, J. Xie, Surface acoustic wave humidity sensors based on uniform and thickness controllable graphene oxide thin films formed by surface tension, 2019/07/29, Microsyst. Nanoeng. vol. 5 (1) (2019) 36, 2019/07/29.
[7] M. Wu, Z. Wu, X. Jin, J.-H. Lee, A highly sensitive FET-Type humidity sensor with inkjet-printed Pt-In2O3 nanoparticles at room temperature, 2020/10/14, Nanoscale Res. Lett. vol. 15 (1) (2020) 198, 2020/10/14.
[8] F. Fauzi, A. Rianjanu, I. Santoso, K. Triyana, Gas and humidity sensing with quartz crystal microbalance (QCM) coated with graphene-based materials - a mini review, 2021/10/15/, Sens. Actuators A Phys. vol. 330 (2021), 112837, 2021/10/15/.
[9] J. Xu, M. Bertke, H.S. Wasisto, E. Peiner, Piezoresistive microcantilevers for humidity sensing, 2019/04/04, J. Micromech. Microeng. vol. 29 (5) (2019), 053003, 2019/04/04.
[10] H. Muñoz-Galán, C. Alemán, M.M. Pérez-Madrigal, Beyond biology: alternative uses of cantilever-based technologies, Lab a Chip vol. 23 (5) (2023) 1128–1150.
[11] A. Ahmad, Z. Adnan, A. Abdulrahman, MEMS Humidity Sensors, p. Ch. 4, in: C. Muhammad Tariq Saeed, A. Abdullah Mohammed, K. Sher Bahadar (Eds.), Humidity Sensors, IntechOpen, Rijeka, 2021.
[12] S. Goel, P. Khanduri, V. Panwar, S. Chauhan, Synthesis and characterization of polymer based humidity sensor, 2022/11/08, AIP Conf. Proc. vol. 2481 (1) (2022), 020024, 2022/11/08.
[13] M.U. Khan, G. Hassan, J. Bae, Bio-compatible organic humidity sensor based on natural inner egg shell membrane with multilayer crosslinked fiber structure, 2019/04/09, Sci. Rep. vol. 9 (1) (2019) 5824, 2019/04/09.
[14] M.U. Khan, G. Hassan, M. Awais, J. Bae, All printed full range humidity sensor based on Fe2O3, 2020/08/15/, Sens. Actuators A Phys. vol. 311 (2020), 112072, 2020/08/15/.
[15] I.A. Anisimov, R.W. Evitts, D.E. Cree, L.D. Wilson, Renewable hybrid biopolymer/polyaniline composites for humidity sensing, 2022/10/14, ACS Appl. Polym. Mater. vol. 4 (10) (2022) 7204–7216, 2022/10/14.
[16] C.M. Furqan, M.U. Khan, M. Awais, F. Jiang, J. Bae, A. Hassan, H.-S. Kwok, Humidity sensor based on Gallium Nitride for real time monitoring applications, 2021/05/27, Sci. Rep. vol. 11 (1) (2021) 11088, 2021/05/27.
[17] M.U. Khan, M. Awais, T.E. Chattha, A. Hassan, J. Bae, All printed wide range humidity sensor array combining MoSe2 and PVOH in series, 2020/05/01, J. Mater. Sci. Mater. Electron. vol. 31 (10) (2020) 7683–7697, 2020/05/01.
[18] M.U. Khan, G. Hassan, R.A. Shaukat, Q.M. Saqib, M.Y. Chougale, J. Kim, J. Bae, Wide range and highly linear signal processed systematic humidity sensor array using methylene blue and graphene composite, 2021/08/17, Sci. Rep. vol. 11 (1) (2021) 16665, 2021/08/17.
[19] M. Khalifa, G. Wuzella, H. Lammer, A.R. Mahendran, Smart paper from graphene coated cellulose for high-performance humidity and piezoresistive force sensor, 2020/08/01/, Synth. Met. vol. 266 (2020), 116420, 2020/08/01/.
[20] P. Zhu, H. Ou, Y. Kuang, L. Hao, J. Diao, G. Chen, Cellulose nanofiber/carbon nanotube dual network-enabled humidity sensor with high sensitivity and durability, 2020/07/22, ACS Appl. Mater. Interfaces vol. 12 (29) (2020) 33229–33238, 2020/07/22.
[21] R. Alrammouz, J. Podlecki, A. Vena, R. Garcia, P. Abboud, R. Habchi, B. Sorli, Highly porous and flexible capacitive humidity sensor based on self-assembled graphene oxide sheets on a paper substrate, 2019/11/01/, Sens. Actuators B Chem. vol. 298 (2019), 126892, 2019/11/01/.
[22] D.-D. Han, Y.-L. Zhang, H.-B. Jiang, H. Xia, J. Feng, Q.-D. Chen, H.-L. Xu, H.-B. Sun, Moisture-responsive graphene paper prepared by self-controlled photoreduction, 2015/01/01, Adv. Mater. vol. 27 (2) (2015) 332–338, 2015/01/01.
[23] P. Zhu, Y. Kuang, Y. Wei, F. Li, H. Ou, F. Jiang, G. Chen, Electrostatic self-assembly enabled flexible paper-based humidity sensor with high sensitivity and superior durability, 2021/01/15/, Chem. Eng. J. vol. 404 (2021), 127105, 2021/01/15/.
[24] Y. Yang, G. Su, Q. Li, Z. Zhu, S. Liu, B. Zhuo, X. Li, P. Ti, Q. Yuan, Performance of the highly sensitive humidity sensor constructed with nanofibrillated cellulose/graphene oxide/polydimethylsiloxane aerogel via freeze drying, RSC Adv. vol. 11 (3) (2021) 1543–1552.
[25] A. Chaim, H. Abunahla, B. Mohammad, N. Alamoodi, and A. Alazzam, "PrMem: Novel flexible biodegradable paper-graphene oxide-based memristor," *MRS Bulletin*, 2022/09/28, 2022.

[26] Y. Abbas, M. Rezeq, A. Nayfeh, I. Saadat, Size dependence of charge retention in gold-nanoparticles sandwiched between thin layers of titanium oxide and silicon oxide, 2021/10/18, Appl. Phys. Lett. vol. 119 (16) (2021), 162103, 2021/10/18.
[27] M. Rezeq, Y. Abbas, B. Wen, Z. Wasilewski, D. Ban, Direct detection of electronic states for individual indium arsenide (InAs) quantum dots grown by molecular beam epitaxy, 2022/07/15/, Appl. Surf. Sci. vol. 590 (2022), 153046, 2022/07/15/.
[28] S. Thakur, N. Karak, Green reduction of graphene oxide by aqueous phytoextracts, 2012/11/01/, Carbon vol. 50 (14) (2012) 5331–5339, 2012/11/01/.
[29] N.M.S. Hidayah, W.-W. Liu, C.-W. Lai, N.Z. Noriman, C.-S. Khe, U. Hashim, H. C. Lee, Comparison on graphite, graphene oxide and reduced graphene oxide: synthesis and characterization, 2017/10/16, AIP Conf. Proc. vol. 1892 (1) (2017), 150002, 2017/10/16.
[30] W. Liu, G. Speranza, Tuning the oxygen content of reduced graphene oxide and effects on its properties, 2021/03/09, ACS Omega vol. 6 (9) (2021) 6195–6205, 2021/03/09.
[31] R.A. Shaukat, M.U. Khan, Q.M. Saqib, M.Y. Chougale, J. Kim, J. Bae, All range highly linear and sensitive humidity sensor based on 2D material TiSi2 for real-time monitoring, 2021/10/15/, Sens. Actuators B Chem. vol. 345 (2021), 130371, 2021/10/15/.
[32] R.A. Shaukat, M.U. Khan, Q.M. Saqib, M.Y. Chougale, J. Kim, A. Bermak, J. Bae, Two dimensional Zirconium diselenide based humidity sensor for flexible electronics, 2022/05/01/, Sens. Actuators B Chem. vol. 358 (2022), 131507, 2022/05/01/.
[33] Y. Liang, F. Zhao, Z. Cheng, Q. Zhou, H. Shao, L. Jiang, L. Qu, Self-powered wearable graphene fiber for information expression, 2017/02/01/, Nano Energy vol. 32 (2017) 329–335, 2017/02/01/.
[34] D. Lei, Q. Zhang, N. Liu, T. Su, L. Wang, Z. Ren, Z. Zhang, J. Su, Y. Gao, Self-powered graphene oxide humidity sensor based on potentiometric humidity transduction mechanism, 2022/03/01, Adv. Funct. Mater. vol. 32 (10) (2022) 2107330, 2022/03/01.
[35] R.K. Jha, P.K. Guha, Liquid exfoliated pristine WS2 nanosheets for ultrasensitive and highly stable chemiresistive humidity sensors, 2016/10/24, Nanotechnology vol. 27 (47) (2016), 475503, 2016/10/24.
[36] S.-L. Zhang, H. Jung, J.-S. Huh, J.-B. Yu, W.-C. Yang, Efficient exfoliation of MoS2 with volatile solvents and their application for humidity sensor, J. Nanosci. Nanotechnol. vol. 14 (11) (2014) 8518–8522.
[37] Y. Guo, K. Xu, C. Wu, J. Zhao, Y. Xie, Surface chemical-modification for engineering the intrinsic physical properties of inorganic two-dimensional nanomaterials, Chem. Soc. Rev. vol. 44 (3) (2015) 637–646.
[38] H. Huang, A. Sun, C. Chu, Y. Li, G. Xu, Electrical and humidity sensing properties of graphene and polystyrene sulfonic sodium bilayer thin film, 2013/01/01, Integr. Ferroelectr. vol. 144 (1) (2013) 127–134, 2013/01/01.
[39] J. Xu, and E. Peiner, "Micromachined Silicon Cantilever Resonator-Based Humidity Sensors for Multifunctional Applications." pp. 326–329.
[40] B. Li, Q. Tian, H. Su, X. Wang, T. Wang, D. Zhang, High sensitivity portable capacitive humidity sensor based on In2O3 nanocubes-decorated GO nanosheets and its wearable application in respiration detection, 2019/11/15/, Sens. Actuators B: Chem. vol. 299 (2019), 126973, 2019/11/15/.
[41] D. Zhang, Z. Xu, Z. Yang, X. Song, High-performance flexible self-powered tin disulfide nanoflowers/reduced graphene oxide nanohybrid-based humidity sensor driven by triboelectric nanogenerator, 2020/01/01/, Nano Energy vol. 67 (2020), 104251, 2020/01/01/.
[42] L. Lan, X. Le, H. Dong, J. Xie, Y. Ying, J. Ping, One-step and large-scale fabrication of flexible and wearable humidity sensor based on laser-induced graphene for real-time tracking of plant transpiration at bio-interface, 2020/10/01/, Biosens. Bioelectron. vol. 165 (2020), 112360, 2020/10/01/.
[43] J. Wu, Z. Wu, H. Ding, Y. Wei, X. Yang, Z. Li, B.-R. Yang, C. Liu, L. Qiu, X. Wang, Multifunctional and high-sensitive sensor capable of detecting humidity, temperature, and flow stimuli using an integrated microheater, 2019/11/20, ACS Appl. Mater. Interfaces vol. 11 (46) (2019) 43383–43392, 2019/11/20.
[44] S.-J. Choi, H. Yu, J.-S. Jang, M.-H. Kim, S.-J. Kim, H.S. Jeong, I.-D. Kim, Nitrogen-doped single graphene fiber with platinum water dissociation catalyst for wearable humidity sensor, 2018/03/01, Small vol. 14 (13) (2018) 1703934, 2018/03/01.
[45] D. Zhang, J. Tong, B. Xia, Humidity-sensing properties of chemically reduced graphene oxide/polymer nanocomposite film sensor based on layer-by-layer nano self-assembly, 2014/07/05/, Sens. Actuators B Chem. vol. 197 (2014) 66–72, 2014/07/05/.
[46] R. Jalili, D. Esrafilzadeh, S.H. Aboutalebi, Y.M. Sabri, A.E. Kandjani, S.K. Bhargava, E. Della Gaspera, T.R. Gengenbach, A. Walker, Y. Chao, C. Wang, H. Alimadadi, D. R.G. Mitchell, D.L. Officer, D.R. MacFarlane, G.G. Wallace, Silicon as a ubiquitous contaminant in graphene derivatives with significant impact on device performance, 2018/11/29, Nat. Commun. vol. 9 (1) (2018) 5070, 2018/11/29.
[47] Y. Yao, X. Chen, H. Guo, Z. Wu, Graphene oxide thin film coated quartz crystal microbalance for humidity detection, 2011/06/15/, Appl. Surf. Sci. vol. 257 (17) (2011) 7778–7782, 2011/06/15/.
[48] Z. Yuan, H. Tai, Z. Ye, C. Liu, G. Xie, X. Du, Y. Jiang, Novel highly sensitive QCM humidity sensor with low hysteresis based on graphene oxide (GO)/poly (ethyleneimine) layered film, 2016/10/29/, Sens. Actuators B Chem. vol. 234 (2016) 145–154, 2016/10/29/.
[49] C.L. Zhao, M. Qin, W.H. Li, and Q.A. Huang, "Enhanced performance of a CMOS interdigital capacitive humidity sensor by graphene oxide." pp. 1954–1957.
[50] Y. Yao, X. Chen, H. Guo, Z. Wu, X. Li, Humidity sensing behaviors of graphene oxide-silicon bi-layer flexible structure, 2012/01/03/, Sens. Actuators B Chem. vol. 161 (1) (2012) 1053–1058, 2012/01/03/.
[51] S.I. Jung, I.R. Jang, C. Ryu, J. Park, A.M. Padhan, H.J. Kim, Graphene oxide decorated multi-frequency surface acoustic wave humidity sensor for hygienic applications, 2023/04/26, Sci. Rep. vol. 13 (1) (2023) 6838, 2023/04/26.
[52] D. Li, X. Le, J. Pang, and J. Xie, "An ALN Resonant Microcantilever Humidity Sensor by Activating Specific Sets of Top Electrodes Based on Graphene Oxide." pp. 1337–1340.
[53] X. Le, F. Ma, D. Li, J. Pang, Z. Xu, C. Gao, and J. Xie, An improved sensitivity AlN microcantilever humidity sensor using interdigital transducers actuated very high resonant mode and graphene oxide sensing layer pp. 928–931.
[54] X. Le, L. Peng, J. Pang, Z. Xu, C. Gao, J. Xie, Humidity sensors based on AlN microcantilevers excited at high-order resonant modes and sensing layers of uniform graphene oxide, 2019/03/15/, Sens. Actuators B Chem. vol. 283 (2019) 198–206, 2019/03/15/.
[55] J. Pang, X. Le, K. Pang, Z. Xu, C. Gao, J. Xie, Modified coefficient of equivalent mass to explain decreased relative sensitivity of piezoelectric cantilever humidity sensor in high mode, J. Micro Syst. vol. 29 (4) (2020) 452–454.

Dr. Muhammad Umair Khan received his Ph.D. as an ocean system engineering major (Material and Electronic System Engineering Track) from Jeju National University, South Korea, in 2022. Since 2022, he has been a postdoctoral fellow in Khalifa University of Science and Technology. His major areas of research include nanogenerators, memristors, biosensors, humidity sensors, photosensors, material processing and fabrication, and characterization of all printed circuits.

Dr. Yawar Abbas is a research scientist at the Department of Physics, Khalifa University, Abu Dhabi, UAE. Before joining Khalifa University, he was a postdoctoral research fellow at Hanyang University, Seoul, South Korea, where he worked on the crossbar arrays of Resistive Random Access Memory (RRAM) and its neuromorphic applications. His research interests include nanoscale memory devices for neuromorphic applications, failure analysis of semiconductor devices and nanoscale probing using an atomic force microscope.

Dr. Heba Abunahla earned her Ph.D. from Khalifa University, Abu Dhabi, UAE. Dr. Heba is an Assistant Professor at the Quantum and Computer Engineering Department, Delft University of Technology, Delft, Netherlands. Before joining Delft University of Technology, she was a Research Scientist at the Department of Electrical Engineering and Computer Sciences, where she developed reduced graphene oxide-based memristive devices for neuromorphic computing. She has more than 7 years of experience in fabrication and characterization of semiconductor devices like memristors and sensors.

Dr. Moh'd Rezeq is an Associate Professor at the Department of Physics. He has a long experience in the nanotechnology field. He has established a nanofabrication and nano-probe lab at Khalifa University (KU) with the capability of fabricating and characterizing nanomaterials at sub-1 nm scale. His research is dedicated to low-power and energy-efficient nano-devices.

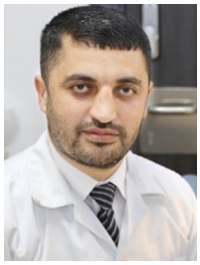

Dr. Anas Alazzam is an alumnus of Concordia University—Montreal, Canada. After a brief post-doctoral fellow appointment with the Canadian Space Agency, he joined Khalifa University in 2012. He is currently an associate professor of Mechanical Engineering and the head of the Microfluidics lab at Khalifa University. He has research background in microfluidics, nanofluids, dielectrophoresis, microsystems, phase change materials, and healthcare applications of microdevices. His research has received substantial recognition in the form of awards and media appearance. He is a member of the editorial board of Micromachines and PLOS ONE Journals.

Dr. Baker Mohammad, a professor of Electrical Engineering and Computer Science (EECS) at Khalifa University, holds the position of Director of the System at the Chip Center. He earned his PhD from the University of Texas at Austin. With a distinguished career spanning 16 years in leading technology companies such as Intel Corporation and Qualcomm Incorporated, Dr. Mohammad has honed his expertise in microprocessor design, focusing on memory, low-power circuit, and physical design. His research interests encompass a broad spectrum of topics, including VLSI, power-efficient computing, high-yield embedded memory, and emerging technologies such as Memristor, STTRAM, and In-Memory Computing. As part of his role at Khalifa University, Dr. Mohammad spearheads the development of low-power SOC and hardware accelerators for Cyber-Physical Systems.

Dr. Nahla Alamoodi is an Assistant Professor of Chemical Engineering at Khalifa University. She received her PhD degree from the University of Minnesota, USA, in 2016. Her research interests are in conventional and paper-based microfluidics with focus on surface functionalization, separation of multiphase systems, and sensing applications. She is currently a member of the research and innovation on Carbon and Hydrogen Center (RICH), Center of Catalysis and Separation (CeCaS), and System on Chip Lab (SoCL).